General quantum theory of nonlinear optical-pulse propagation

Yinchieh Lai and Shinn-Sheng Yu
Institute of Electro-Optical Engineering, National Chiao-Tung University, Hsinchu, Taiwan, Republic of China
(Received 7 February 1994; revised manuscript received 2 August 1994)

Based on the linearization approximation and the conservation of commutation brackets, a general, self-consistent scheme is developed to quantize nonlinear optical-pulse propagation problems. A general computation procedure is developed to calculate the quantum uncertainties of the inner product between any given function and the (perturbed) field operator. As an illustration, a self-consistent quantum theory of the self-Raman effect in optical fibers is presented. The influence of the self-Raman effect on soliton squeezing is examined.

PACS number(s): 42.50.Dv, 42.65.Dr, 42.81.Dp

I. INTRODUCTION

The advance of technology has led to the possibility of studying quantum effects of optical-pulse propagation inside nonlinear media. Recent experiments on generating pulse squeezed states using optical fibers [1–3] are good examples of experimental efforts in this direction. Because of this, the development of a satisfactory quantum theory of nonlinear optical-pulse propagation has attracted a lot of attention recently. In the literature, quantum effects of pulse propagation inside dispersionless Kerr media have been studied by many authors [4–7]. Quantum effects of soliton propagation in optical fibers have also been examined by many approaches [8–14]. Through the studies of these systems, we have gained a lot of understanding of the quantum nature of nonlinear pulse propagation. It is natural to generalize the treatment to more complicated nonlinear pulse propagation problems. The quantum effects of third-order dispersion have been studied using the time-dependent Hartree approximation [15]. A quantum theory of the self-Raman effect has been developed using a Hamiltonian approach [16,17]. However, to proceed further in this direction, there are still two important missing links that must be filled. First of all, the systems to be studied may not be Hamiltonian systems and then their quantization may become a problem. We need a general quantization scheme. Second, it is quite possible that the systems to be studied can no longer be solved analytically. We need a general computational procedure to calculate quantum uncertainties.

About the first missing link, a solvable example of non-Hamiltonian systems is the self-induced transparency solitons [18]. In one of our previous works, we have successfully quantized and solved this problem using the linearization approach and by taking advantage of the fact that the classical self-induced transparency problem can be solved analytically using an inverse scattering transform. In fact, the method we developed there is already applicable to any problem that can be solved by the Zakharov-Shabat inverse scattering transform. However, in dealing with more general systems, we may not have the same luck that the classical solution is known analytically. Therefore we still need to seek a quantization scheme that can be applied to general problems.

About the second missing link, one possible solution is to transform the quantum operator equations into equivalent stochastic equations by using positive-P representation and then to solve the stochastic equations by direct numerical simulation. This approach has been demonstrated to work on Hamiltonian systems, such as the nonlinear Schrödinger equation [9,10], and is applicable to other Hamiltonian or non-Hamiltonian systems as long as the quantization problem can be solved. Alternatively, the Wigner representation can also be used to derive approximate equivalent stochastic equations. Such a method has been used to study the impact of Raman effects on soliton squeezing [17]. Even though the above approach is very general, the procedure for transforming quantum problems into stochastic problems is not easy to follow and direct numerical simulation requires a lot of computation to achieve good accuracy. We still need a simple, yet general, computation procedure for calculating quantum uncertainties.

The objective of the present paper is to offer a simple solution to the two missing links mentioned above. Based on the linearization approximation and the conservation of commutation brackets, a general, self-consistent scheme is developed to quantize general nonlinear optical-pulse propagation problems. Quantization based on the preservation of commutator brackets has been widely used in the quantum treatment of linear optical loss and optical gain [19]. It represents a straightforward approach to quantize linear systems. In combination with the linearization approximation, we generalize the approach to nonlinear systems. This is the subject of Sec. II. In Sec. III we develop a general computation procedure ("the backpropagation method") to calculate the quantum uncertainties of the inner product between any given function and the (perturbed) field operator. This general computation procedure is a generalization of the method we developed previously for noise analyses of soliton propagation [14,20]. However, it is not limited to solitons; it is now applicable to general nonlinear pulse propagation problems. Finally, in Sec. IV we take the self-Raman effect in optical fibers [21,22] as an ex-

ample to illustrate our theory. A quantum treatment of the self-Raman effect in optical fibers can be found in Refs. [16,17]. Here we present a different approach. The quantization is based on the preservation of commutation brackets and the calculation of quantum uncertainties is based on the backpropagation method. The influence of the self-Raman effect on soliton squeezing is then examined.

II. GENERAL SCHEME OF QUANTIZATION

A classical complex nonlinear optical-pulse propagation equation can be written generally as

$$\frac{\partial}{\partial z}U(z,t) = F(U(z,t), U^*(z,t)). \tag{2.1}$$

Here $U(z,t)$ is the normalized optical field envelope function, z is the propagation distance, t is time, and $F(\,)$ is a nonlinear function of U, U^*, and their derivatives or integrals with respect to t. The optical field is normalized in such a way that $\int |U(z,t)|^2 dt$ represents the total photon number in the optical pulse at the propagation distance z.

If $U_0(z,t)$ is the exact solution of Eq. (2.1), then the evolution equation of the perturbation field $u(z,t)$ can be obtained by the standard linearization procedure. Setting

$$U(z,t) = U_0(z,t) + u(z,t), \tag{2.2}$$

substituting Eq. (2.2) into Eq. (2.1), expanding in a Taylor series, and ignoring all the higher-order terms of u and u^*, one obtains a linear equation with the general form

$$\frac{\partial}{\partial z}u(z,t) = P_1(z,t)u(z,t) + P_2(z,t)u^*(z,t). \tag{2.3}$$

Here $P_1(z,t)$ and $P_2(z,t)$ are complex differential and integral operators, respectively (on t), that may depend on U_0.

We are now going to quantize the problem using the linear equation Eq. (2.3) instead of the nonlinear equation Eq. (2.1). Of course this is an approximation. However, it is a very good one since usually quantum uncertainties are much smaller compared to the mean values of the field and thus the contributions of higher-order terms are very small. Our previous studies on the nonlinear Schrödinger equation and the self-induced transparency problem based on this approach have been proven to be very successful. This represents a straightforward approach to quantize nonlinear optical-pulse propagation problems.

Quantization is performed by imposing the following commutation relations for the perturbation fields $u(z,t)$ and $u^*(z,t)$:

$$[\hat{u}(z,t_1), \hat{u}^\dagger(z,t_2)] = \delta(t_1 - t_2), \tag{2.4}$$

$$[\hat{u}(z,t_1), \hat{u}(z,t_2)] = [\hat{u}^\dagger(z,t_1), \hat{u}^\dagger(z,t_2)] = 0. \tag{2.5}$$

Equations (2.4) and (2.5) are the commonly used commutation relations for the photon field. We have used $\hat{u}$ and $\hat{u}^\dagger$ instead of u and u^* to denote that they are now quantum operators. With these new notations, Eq. (2.3) now becomes

$$\frac{\partial}{\partial z}\hat{u}(z,t) = P_1(z,t)\hat{u}(z,t) + P_2(z,t)\hat{u}^\dagger(z,t) + \hat{n}(z,t). \tag{2.6}$$

In Eq. (2.6) we have also introduced an additional zero-mean noise operator $\hat{n}(z,t)$. The noise operator $\hat{n}(z,t)$ is assumed to be δ-function correlated in z and with the commutation relations

$$[\hat{n}(z,t_1), \hat{n}^\dagger(z',t_2)] = N(z,t_1,t_2)\delta(z-z'), \tag{2.7}$$

$$[\hat{n}(z,t_1), \hat{n}(z',t_2)] = [\hat{n}^\dagger(z,t_1), \hat{n}^\dagger(z',t_2)] = 0. \tag{2.8}$$

Here $N(z,t_1,t_2)$ has to be chosen correctly so that the commutation relations Eqs. (2.4) and (2.5) are satisfied for all z. The preservation of commutation brackets is a fundamental requirement of quantum mechanics. In the Appendix we show that this requirement implies

$$\begin{aligned} N(z,t_1,t_2) &= \{ -P_1(z,t_1) - P_1^*(z,t_2)\}\delta(t_1-t_2) \\ &\equiv N_D(z,t_1,t_2)\delta(t_1-t_2). \end{aligned} \tag{2.9}$$

Please bear in mind that $N_D(z,t_1,t_2) \equiv -P1(z,t_1) - P_1^*(z,t_2)$ is in general a differential or integral operator which operates on a δ function as shown in Eq. (2.9). Therefore, Eq. (2.9) is merely a formal representation and its real meaning can be understood only when it is inserted inside integrals.

After successfully introducing noise operators to preserve commutation brackets, we have quantized the problem self-consistently by deriving a self-consistent operator equation. Such a quantization procedure based on the preservation of commutator brackets has been widely used in the quantum treatment of linear optical loss and optical gain [19]. It represents a straightforward approach to quantize linear systems. In the present paper we apply it to quantize nonlinear systems with the help of the linearization approximation.

Knowing the commutation brackets is not sufficient for determining quantum uncertainties. From Eqs. (2.7) and (2.8) one can only induce that

$$\begin{aligned} &\langle[\hat{n}(z,t_1), \hat{n}^\dagger(z',t_2)]\rangle \\ &\quad = \langle \hat{n}(z,t_1)\hat{n}^\dagger(z',t_2)\rangle - \langle \hat{n}^\dagger(z',t_2)\hat{n}(z,t_1)\rangle \\ &\quad = N(z,t_1,t_2)\delta(z-z'). \end{aligned} \tag{2.10}$$

To calculate quantum uncertainties, we need to know all of the four correlation functions: $\langle \hat{n}(z,t_1)\hat{n}(z',t_2)\rangle$,

$$\langle \hat{n}(z,t_1)\hat{n}^\dagger(z',t_2)\rangle, \langle \hat{n}^\dagger(z,t_1)\hat{n}(z',t_2)\rangle,$$

and $\langle \hat{n}^\dagger(z,t_1)\hat{n}^\dagger(z',t_2)\rangle$. This can only be achieved by assuming or knowing more about the properties of noise

sources. For example, in the quantum treatment of linear optical loss, the noise is modeled as coming from the direct coupling to a reservoir composed of a set of harmonic oscillators. If the reservoir is in its ground state, then the noise operators $\hat{n}$ and $\hat{n}^\dagger$ can be interpreted as the annihilation and creation operators, respectively, and thus

$$\langle \hat{n}(z,t_1)\hat{n}(z',t_2)\rangle = \langle \hat{n}^\dagger(z,t_1)\hat{n}^\dagger(z',t_2)\rangle = 0, \quad (2.11)$$

$$\langle \hat{n}(z,t_1)\hat{n}^\dagger(z',t_2)\rangle = N(z,t_1,t_2)\delta(z-z'), \quad (2.12)$$

$$\langle \hat{n}^\dagger(z,t_1)\hat{n}(z',t_2)\rangle = 0. \quad (2.13)$$

If the reservoir is at a temperature T, then Eqs. (2.12) and (2.13) become

$$\langle \hat{n}(z,t_1)\hat{n}^\dagger(z',t_2)\rangle = [n_\Omega(T)+1]N(z,t_1,t_2)\delta(z-z'), \quad (2.14)$$

$$\langle \hat{n}^\dagger(z,t_1)\hat{n}(z',t_2)\rangle = n_\Omega(T)N(z,t_1,t_2)\delta(z-z'). \quad (2.15)$$

Here

$$n_\Omega(T) = \frac{1}{e^{\frac{\hbar\Omega}{kT}}-1} \quad (2.16)$$

is the mean number of quanta of the noise source at temperature T and Ω is the resonance frequency of the harmonic oscillators.

For more complicated problems, it is necessary to examine more carefully the physical origin of the noise before one can determine the correlation functions. A good example is the self-Raman effect in optical fibers, which is treated in Sec. IV.

III. GENERAL SCHEME OF CALCULATING QUANTUM UNCERTAINTIES

In many cases of interest it is sufficient to find the quantum uncertainties of the inner product of a weighting function $f(t)$ with the perturbation field operator $\hat{u}(z,t)$. Here the inner product is defined in the usual way as

$$\langle f(t)|g(t)\rangle \equiv \frac{1}{2}\int [f^*(t)g(t)+f(t)g^*(t)]dt. \quad (3.1)$$

To make the notation more elegant, we will rewrite Eq. (2.6) in a more compact way [20]

$$\frac{\partial}{\partial z}\hat{u}(z,t) = P_1(z,t)\hat{u}(z,t)+P_2(z,t)\hat{u}^\dagger(z,t)+\hat{n}(z,t) \equiv \mathbf{P}(z,t)\bullet\hat{u}(z,t)+\hat{n}(z,t). \quad (3.2)$$

We have put a $\bullet$ after $\mathbf{P}$ to remind readers that the operator $\mathbf{P}$ is a special operator that operates on both $\hat{u}$ and $\hat{u}^\dagger$.

The adjoint operator of $\mathbf{P}$ is defined according to

$$\langle f|\mathbf{P}\bullet g\rangle = \langle \mathbf{P^A}\bullet f|g\rangle. \quad (3.3)$$

For a given problem, the analytical form of the adjoint operator $\mathbf{P^A}$ can be derived easily using the definition Eq. (3.3) with the possible help of integration by parts.

We now define an adjoint system that is described by

$$\frac{\partial}{\partial z}u^A(z,t) = -\mathbf{P^A}(z,t)\bullet u^A(z,t). \quad (3.4)$$

Note that the adjoint system is a classical, deterministic system, whereas the original system is a quantum system. Moreover, it is not difficult to prove that the solutions of the original and the adjoint systems have to satisfy

$$\frac{d}{dz}\langle u^A(z,t)|\hat{u}(z,t)\rangle = \langle u^A(z,t)|\hat{n}(z,t)\rangle. \quad (3.5)$$

Integrating both sides from $z=0$ to $z=L$, one immediately has

$$\langle u^A(L,t)|\hat{u}(L,t)\rangle = \langle u^A(0,t)|\hat{u}(0,t)\rangle + \int_0^L \langle u^A(z,t)|\hat{n}(z,t)\rangle dz. \quad (3.6)$$

From Eq. (3.6), the uncertainties of $\langle u^A(L,t)|\hat{u}(L,t)\rangle$ can be written as

$$\begin{aligned}\mathrm{Var}[\langle u^A(L,t)|\hat{u}(L,t)\rangle] = \mathrm{Var}[\langle u^A(0,t)|\hat{u}(0,t)\rangle] &+ \frac{1}{4}\int_0^L\int_0^L\int\int u^{A*}(z,t_1)u^{A*}(z',t_2)\langle \hat{n}(z,t_1)\hat{n}(z',t_2)\rangle dt_1dt_2dzdz' \\ &+\frac{1}{4}\int_0^L\int_0^L\int\int u^{A*}(z,t_1)u^{A}(z',t_2)\langle \hat{n}(z,t_1)\hat{n}^\dagger(z',t_2)\rangle dt_1dt_2dzdz' \\ &+\frac{1}{4}\int_0^L\int_0^L\int\int u^{A}(z,t_1)u^{A*}(z',t_2)\langle \hat{n}^\dagger(z,t_1)\hat{n}(z',t_2)\rangle dt_1dt_2dzdz' \\ &+\frac{1}{4}\int_0^L\int_0^L\int\int u^{A}(z,t_1)u^{A}(z',t_2)\langle \hat{n}^\dagger(z,t_1)\hat{n}^\dagger(z',t_2)\rangle dt_1dt_2dzdz'. \end{aligned} \quad (3.7)$$

Equation (3.7) is the main result of this section. The first term on the right-hand side is the original uncertainty after being transformed by the nonlinear process. The last four terms are the contributions from the noises added midway. The quantum uncertainties of the projection between a given function $u^A(L,t)$ and the perturbed field operator $\hat{u}(z,t)$ is determined fully by the solution $u^A(z,t)$ of the deterministic adjoint system and the stochastic properties of the noise operator.

Equation (3.7) provides us with a general scheme for calculating quantum uncertainties. The computation procedure is as follows.

(i) Solve the classical nonlinear problem either analytically or numerically to obtain $U_0(z,t)$ for $0 \leq z \leq L$.

(ii) Decide $u^A(L,t)$ according to the purpose of calculation (an example can be found in Sec. IV).

(iii) Backpropagate the adjoint system Eq. (3.4) from $z = L$ to $z = 0$ with the initial condition $u^A(L,t)$.

(iv) Calculate the quantum uncertainties according to Eq. (3.7).

The computation procedure given here is a generalization of the method developed in our previous papers [14,20].

If the classical nonlinear pulse propagation equation has properties of phase-shift invariance or time-shift invariance, then there exist conserved quantities that can be used to check the numerical accuracy of the solution of the adjoint system [20]. Here "phase (time) shift invariance" means that if one shifts the solution of the classical nonlinear equation by a constant phase (time position), the obtained function is also a solution. These conserved quantities prove to be very helpful in our numerical programming.

IV. SELF-RAMAN EFFECT IN OPTICAL FIBERS

The formulation developed in previous sections is applicable to general pulse propagation problems. In this section we take the self-Raman effect in optical fibers as an example for illustration. The study of the self-Raman effect in optical fibers has its own importance in pulse squeezed state generation using optical fibers [1–3]. With a loop interferometer configuration, a pulse squeezed vacuum has been successfully generated at the 1.3-μm wavelength [2,3] and at the 1.55-μm wavelength [1]. In the squeezing experiment at 1.3 μm, pulses from mode-locked Nd:YAG or Nd:YLF lasers with a pulse duration around 20 ps were used. At this wavelength, the group velocity dispersion is close to zero. In the squeezing experiment at 1.55 μm, pulses from a mode-locked color-center laser with a pulse duration around 200 fs were used. The group-velocity dispersion is negative and the pulses propagated inside the optical fiber are actually solitary pulses. In going from longer pulses to shorter pulses, one gains the advantages of a high peak power at the same pulse energy and thus a shorter propagation distance in order to achieve appreciable squeezing. However, it is well known that when the pulse duration is below 1 ps, the self-Raman effect will start to affect pulse propagation. It is thus important to study the influence of the self-Raman effect on the achievable squeezing ratio. In order to do this, one needs a quantum theory of the self-Raman effect in optical fibers.

The self-Raman effect is due to the interaction of photons with optical phonons. In the literature, a quantum theory of the self-Raman effect has been developed using a Hamiltonian approach [16]. The phonon field is assumed to be purely inhomogeneously broadened and the correlation function of the noise operator is derived. One example of the calculation of the squeezing ratio in the presence of the self-Raman effect has also been obtained by direct numerical simulation based on a truncated Wigner representation [17]. In this paper we present a different approach. The quantization is based on the preservation of commutation brackets and the calculation of squeezing is based on our backpropagation method.

We model the self-Raman effect in two ways. In our first model the phonon field is treated as purely homogeneously broadened, while in the second model the phonon field is treated as purely inhomogeneously broadened. The two models represent the two limits. The actual phonon field in optical fibers should be both homogeneously and inhomogeneously broadened. Since optical fibers are not made of crystals, the inhomogeneously broadened mechanism should dominate. Nevertheless, it is of interest to compare the two limits and find out their differences. In the following two subsections we develop a formulation for the two limiting cases. In the third subsection we present our results of the numerical calculation.

A. Self-Raman effect with a homogeneously broadened phonon field

The interaction of photons with homogeneously broadened optical phonons can be modeled as

$$v_c \frac{\partial}{\partial z} U(z,t) + \frac{\partial}{\partial t} U(z,t) = i g_0 [b(z,t) + b^*(z,t)] U(z,t), \tag{4.1}$$

$$\frac{\partial}{\partial t} b(z,t) = -\gamma b(z,t) - i\Omega_0 b(z,t) + i g_0 U^*(z,t) U(z,t). \tag{4.2}$$

Here U is the optical field envelope function, b is the phonon field, v_c is the group velocity of the optical field, Ω_0 is the resonance frequency of the phonon field, and γ is the decay rate of the phonon field (homogeneously broadening). The physical meaning of Eqs. (4.1) and (4.2) is clear. The optical field envelope travels with a group velocity v_c. The phonon field travels with a zero group velocity and experiences a loss. Its carrier frequency is Ω_0. The phonon field modifies the optical refractive index. This is represented by the term on the right-hand side of Eq. (4.1). The optical field excites phonons. This is represented by the last term on the right-hand side of Eq. (4.2). The constant g_0 represents the coupling strength between photons and phonons.

We remove the term $\partial U/\partial t$ in Eqs. (4.1) and (4.2) by changing to a moving frame that travels with speed v_c. The equations become

$$\frac{\partial}{\partial z}U(z,t) = i\frac{g_0}{v_c}[b(z,t)+b^*(z,t)]U(z,t), \tag{4.3}$$

$$\frac{\partial}{\partial t}b(z,t) = -\gamma b(z,t) - i\Omega_0 b(z,t) + ig_0 U^*(z,t)U(z,t). \tag{4.4}$$

Here we still use t as one of the independent variables, although its meaning has changed. From now on the variable t represents the time deviation from the pulse center.

We further eliminate the phonon field by the following procedure. From Eq. (4.4), one has

$$b(z,t) = ig_0\int_{-\infty}^{t}\exp[(-\gamma - i\Omega_0)(t-\tau)] \times U^*(z,\tau)U(z,\tau)d\tau. \tag{4.5}$$

Substituting Eq. (4.5) into Eq. (4.3), one obtains

$$\frac{\partial}{\partial z}U(z,t) = i\left[\int_{-\infty}^{t}h(t-\tau)U^*(z,\tau)U(z,\tau)d\tau\right]U(z,t). \tag{4.6}$$

Here

$$h(t) = 2\frac{g_0^2}{v_c}\exp(-\gamma t)\sin(\Omega_0 t) \quad \text{if } t\geq 0$$
$$= 0 \quad \text{if } t<0. \tag{4.7}$$

Equation (4.6) says that the self-Raman effect can be modeled by a noninstantaneous Kerr nonlinearity [21,22].

In optical fibers, both the group-velocity dispersion and the instantaneous Kerr nonlinearity due to electronic transition exist. Therefore, the complete propagation equation should be

$$\frac{\partial}{\partial z}U(z,t) = id_i\frac{\partial^2}{\partial t^2}U(z,t) + ik_i|U(z,t)|^2U(z,t) + i\left[\int_{-\infty}^{t}h(t-\tau)U^*(z,\tau)U(z,\tau)d\tau\right]U(z,t). \tag{4.8}$$

Here $d_i = -k_0''/2$ represents the group-velocity dispersion and k_i represents the instantaneous Kerr nonlinearity.

Equation (4.8) is a differential-integral equation. In the literature, some authors preferred to use the following partial differential equation to model the self-Raman effect:

$$\frac{\partial}{\partial z}U(z,t) = id_i\frac{\partial^2}{\partial t^2}U(z,t) + ih_0|U(z,t)|^2U(z,t) + ih_1\frac{\partial|U(z,t)|^2}{\partial t}U(z,t). \tag{4.9}$$

Here h_0 and h_1 are two constants. Equation (4.9) can be derived from Eq. (4.8) by expanding $|U(z,\tau)|^2$ around $\tau = t$ to the first order of $\tau - t$. In this way, one obtains the following expressions for h_0 and h_1:

$$h_0 = k_i + \int_0^\infty h(t)dt = k_i + 2\frac{g_0^2}{v_c}\frac{\Omega_0}{\gamma^2+\Omega_0^2} = \frac{\hbar\omega_0 k_0 n_2}{A_{\text{eff}}}, \tag{4.10}$$

$$h_1 = -\int_0^\infty th(t)dt = -4\frac{g_0^2}{v_c}\frac{\gamma\Omega_0}{(\gamma^2+\Omega_0^2)^2}. \tag{4.11}$$

Here A_{eff} is the effective cross section of the fiber, k_0 is the propagation constant, ω_0 is the optical frequency, and n_2 is the usual Kerr coefficient. According to Ref. [22], 82% of the Kerr coefficient comes from the instantaneous Kerr nonlinearity due to an electronic transition [the first term on the right-hand side of Eq. (4.10)], while the other 18% comes from the noninstantaneous Kerr nonlinearity due to a photon-phonon interaction [the second term on the right-hand side of Eq. (4.10)]. Utilizing these results, we estimate the magnitudes of the parameters according to the expressions

$$\gamma = 20 \text{ THz}, \tag{4.12}$$

$$\Omega_0 = 2\pi \times 12 \text{ THz}, \tag{4.13}$$

$$k_i = 0.82\frac{\hbar\omega_0 k_0 n_2}{A_{\text{eff}}}, \tag{4.14}$$

$$2\frac{g_0^2}{v_c}\frac{\Omega_0}{\gamma^2+\Omega_0^2} = 0.18\frac{\hbar\omega_0 k_0 n_2}{A_{\text{eff}}}. \tag{4.15}$$

The approximate equation Eq. (4.9) should be very good when the pulse duration is much longer than the response time of the Raman response function $h(t)$. When the pulse duration is comparable to the response time, the accuracy of such an approximation needs to be checked. In this paper we always use the exact equation Eq. (4.8).

If the quantization procedure in Sec. II is applied to Eq. (4.8), it is not difficult to show that one has to introduce a noise operator $\hat{n}(z,t)$ that obeys the commutation relations given in Eqs. (2.7) and (2.8) by

$$N(z,t_1,t_2) = iU_0(z,t_1)U_0^*(z,t_2)h(t_2-t_1) \quad \text{if } t_2\geq t_1$$
$$= -iU_0(z,t_1)U_0^*(z,t_2)h(t_1-t_2) \quad \text{if } t_2<t_1. \tag{4.16}$$

As we have mentioned before, knowing the commutation relations is not sufficient for calculating quantum uncertainties. We have to examine the origin of the noise more carefully in order to determine all four correlation functions. Physically, the noise comes from the decay of the phonon field. Therefore, it is more physical to go back

to Eq. (4.4) and introduce a noise operator there. After doing this, the quantum operator equations for the self-Raman effect are now given by

$$\frac{\partial}{\partial z}\hat{U}(z,t) = id_i\frac{\partial^2}{\partial t^2}\hat{U}(z,t) + ik_i\hat{U}^\dagger(z,t)\hat{U}(z,t)\hat{U}(z,t) + i\frac{g_0}{v_c}[\hat{b}(z,t)+\hat{b}^\dagger(z,t)]\hat{U}(z,t), \quad (4.17)$$

$$\frac{\partial}{\partial t}\hat{b}(z,t) = -\gamma\hat{b}(z,t) - i\Omega_0\hat{b}(z,t) + ig_0\hat{U}^\dagger(z,t)\hat{U}(z,t) + \hat{n}_b(z,t). \quad (4.18)$$

Here we have also included the group-velocity dispersion and the instantaneous Kerr nonlinearity terms.

By eliminating the phonon field again, we get

$$\frac{\partial}{\partial z}\hat{U}(z,t) = id_i\frac{\partial^2}{\partial t^2}\hat{U}(z,t) + ik_i\hat{U}^\dagger(z,t)\hat{U}(z,t)\hat{U}(z,t) + i\left[\int_{-\infty}^{t} h(t-\tau)\hat{U}^\dagger(z,\tau)\hat{U}(z,\tau)d\tau\right]\hat{U}(z,t) + i\int_{-\infty}^{t}[H(t-\tau)\hat{n}_b(z,\tau) + H^*(t-\tau)\hat{n}_b^\dagger(z,\tau)]d\tau\hat{U}(z,t). \quad (4.19)$$

Here

$$H(t) = \frac{g_0}{v_c}\exp[(-\gamma - i\Omega_0)t]. \quad (4.20)$$

By linearizing Eq. (4.19), one obtains an expression for the final noise operator $\hat{n}$ in terms of $\hat{n}_b$,

$$\hat{n}(z,t) = i\int_{-\infty}^{t}[H(t-\tau)\hat{n}_b(z,\tau) + H^*(t-\tau)\hat{n}_b^\dagger(z,\tau)]d\tau U_0(z,t). \quad (4.21)$$

The commutation relations of $\hat{n}_b$ have to be chosen correctly such that the self-consistency requirement Eq. (4.16) is satisfied. This can be achieved by choosing

$$[\hat{n}_b(z,t_1),\hat{n}_b(z',t_2)] = [\hat{n}_b^\dagger(z,t_1),\hat{n}_b^\dagger(z',t_2)] = 0, \quad (4.22)$$

$$[\hat{n}_b(z,t_1),\hat{n}_b^\dagger(z',t_2)] = 2\gamma v_c\delta(t_1-t_2)\delta(z-z'). \quad (4.23)$$

The expression Eq. (4.23) has good physical meanings. The commutator brackets of $\hat{n}_b$ and $\hat{n}_b^\dagger$ is δ-function correlated on time and is proportional to 2γ, as in the usual quantum treatment of a harmonic oscillator with a linear loss. However, in the pulse propagation problem, the commutator brackets of $\hat{n}_b$ and $\hat{n}_b^\dagger$ are also δ-function correlated on space and are proportional to v_c, the relative traveling speed between the light field and the phonon field.

Physically, since the origin of $\hat{n}_b$ is due to the decay of the phonon field, from the quantum treatment of linear loss, we can interpret $\hat{n}_b$ and $\hat{n}_b^\dagger$ as the annihilation and creation operators, respectively, and determine their correlation functions as

$$\langle\hat{n}_b(z,t_1)\hat{n}_b(z',t_2)\rangle = \langle\hat{n}_b^\dagger(z,t_1)\hat{n}_b^\dagger(z',t_2)\rangle = 0, \quad (4.24)$$

$$\langle\hat{n}_b(z,t_1)\hat{n}_b^\dagger(z',t_2)\rangle = 2[n_{\Omega_0}(T)+1]\gamma v_c\delta(t_1-t_2)\delta(z-z'), \quad (4.25)$$

$$\langle\hat{n}_b^\dagger(z,t_1)\hat{n}_b(z',t_2)\rangle = 2n_{\Omega_0}(T)\gamma v_c\delta(t_1-t_2)\delta(z-z'). \quad (4.26)$$

Here

$$n_{\Omega_0}(T) = \frac{1}{e^{\frac{\hbar\Omega_0}{kT}}-1} \quad (4.27)$$

is the mean phonon number at temperature T.

After obtaining the correlation functions of $\hat{n}_b$, the correlation functions of the final noise operator $\hat{n}$ also can be calculated. The results are

$$\langle\hat{n}(z,t_1)\hat{n}(z',t_2)\rangle = -U_0(z,t_1)U_0(z,t_2)N_n(t_1-t_2)\delta(z-z'), \quad (4.28)$$

$$\langle\hat{n}(z,t_1)\hat{n}^\dagger(z',t_2)\rangle = U_0(z,t_1)U_0^*(z,t_2)N_n(t_1-t_2)\delta(z-z'), \quad (4.29)$$

$$\langle\hat{n}^\dagger(z,t_1)\hat{n}(z',t_2)\rangle = U_0^*(z,t_1)U_0(z,t_2)N_n(t_1-t_2)\delta(z-z'), \quad (4.30)$$

$$\langle\hat{n}^\dagger(z,t_1)\hat{n}^\dagger(z',t_2)\rangle = -U_0^*(z,t_1)U_0^*(z,t_2)N_n(t_1-t_2)\delta(z-z'). \quad (4.31)$$

Here the function $N_n(t)$ is given by

$$N_n(t) = \frac{g_0^2}{v_c}\exp(-\gamma|t|)\{[n_{\Omega_0}(T)+1]\exp(-i\Omega_0 t) + n_{\Omega_0}(T)\exp(i\Omega_0 t)\}. \quad (4.32)$$

Up to this point we have successfully quantized the problem in which the phonon field is purely homogeneously broadened.

B. Self-Raman effect with an inhomogeneously broadened phonon field

The interaction of photons with inhomogeneously broadened optical phonons can be modeled as

$$\frac{\partial}{\partial z}\hat{U}(z,t) = id_i\frac{\partial^2}{\partial t^2}\hat{U}(z,t) + ik_i\hat{U}^\dagger(z,t)\hat{U}(z,t)\hat{U}(z,t) + i\int_0^\infty \frac{g(\Omega)}{v_c}[\hat{b}_\Omega(z,t)+\hat{b}_\Omega^\dagger(z,t)]d\Omega\hat{U}(z,t), \tag{4.33}$$

$$\frac{\partial}{\partial t}\hat{b}_\Omega(z,t) = -i\Omega\hat{b}_\Omega(z,t) + ig(\Omega)\hat{U}^\dagger(z,t)\hat{U}(z,t). \tag{4.34}$$

Here the phonon field is now a sum of distributed components with different resonance frequencies. The coupling strength between the photon field and different phonon components are given by a real function $g(\Omega)$. As we are going to see, $2\pi g^2(\Omega)/v_c$ is the Raman gain (in real units) defined in the literature [21,22]. Since each phonon component is assumed to be lossless (no homogeneous broadening), there is no additional noise operator in Eq. (4.34).

We eliminate the phonon field by the following procedure. From Eq. (4.34), one has

$$\hat{b}_\Omega(z,t) = \hat{b}_\Omega(z,-\infty)\exp(-i\Omega t) + ig(\Omega)\int_{-\infty}^t \exp[-i\Omega(t-\tau)]\hat{U}^\dagger(z,\tau)\hat{U}(z,\tau)d\tau. \tag{4.35}$$

Note that the contribution from the initial phonon field component $\hat{b}_\Omega(z,-\infty)$ cannot be ignored in this case, whereas it has been ignored in Eq. (4.5) due to the exponential decay term. In the case of inhomogeneous broadening, the initial phonon field component $\hat{b}_\Omega(z,-\infty)$ does not decay and actually is the noise source.

Substituting Eq. (4.35) into Eq. (4.33), one obtains

$$\frac{\partial}{\partial z}\hat{U}(z,t) = id_i\frac{\partial^2}{\partial t^2}\hat{U}(z,t) + ik_i\hat{U}^\dagger(z,t)\hat{U}(z,t)\hat{U}(z,t) + i\left[\int_{-\infty}^t h(t-\tau)\hat{U}^\dagger(z,\tau)\hat{U}(z,\tau)d\tau\right]\hat{U}(z,t) + i\int_0^\infty \frac{g(\Omega)}{v_c}\{\hat{b}_\Omega(z,-\infty)\exp(-i\Omega t)+\hat{b}_\Omega^\dagger(z,-\infty)\exp(i\Omega t)\}d\Omega\hat{U}(z,t). \tag{4.36}$$

Here the response function $h(t)$ is now given by

$$h(t) = \begin{cases} \frac{2}{v_c}\int_0^\infty g^2(\Omega)\sin(\Omega t)d\Omega & \text{if } t \geq 0 \\ 0 \quad \text{if } t < 0\,. \end{cases} \tag{4.37}$$

The Raman gain is defined as twice the imaginary part of the Fourier transform of $h(t)$ [21,22]:

$$A_R(\Omega) \equiv 2\mathrm{Im}\left[\int h(t)\exp(i\Omega t)dt\right] = \frac{2\pi g^2(\Omega)}{v_c}. \tag{4.38}$$

From this equation, the function $g^2(\Omega)$ can be determined from the experimentally measured Raman gain spectrum [21,22]. This is of course the right approach if one wants to make a very careful comparison with experimental results. Nevertheless, it is also interesting to note that if one assumes a Lorentzian distribution of Raman gain

$$A_R(\Omega) = \frac{2g_0^2}{v_c}\left[\frac{\gamma}{\gamma^2+(\Omega-\Omega_0)^2} - \frac{\gamma}{\gamma^2+(\Omega+\Omega_0)^2}\right], \tag{4.39}$$

then $h(t)$, given by Eq. (4.37), is equal to $h(t)$ in the case of homogeneous broadening [Eq. (4.7)]. In other words, under the assumption of a Lorentzian distribution of the Raman gain, the propagation equation with an inhomogeneously broadened phonon field is identical to the propagation equation with a homogeneously broadened phonon field, except for the noise term.

The preservation of commutation brackets again helps us to determine the right commutation relations for $\hat{b}_\Omega(z,-\infty)$ and $\hat{b}_\Omega^\dagger(z,-\infty)$,

$$[\hat{b}_\Omega(z,-\infty),\hat{b}_{\Omega'}(z',-\infty)] = [\hat{b}_\Omega^\dagger(z,-\infty),\hat{b}_{\Omega'}^\dagger(z',-\infty)] = 0, \tag{4.40}$$

$$[\hat{b}_\Omega(z,-\infty),\hat{b}_{\Omega'}^\dagger(z',-\infty)] = v_c\delta(\Omega-\Omega')\delta(z-z'). \tag{4.41}$$

These are again the right expressions one would expect.

Following a similiar derivation as in the case of homogeneous broadening, we find that the correlation functions of the final noise operator $\hat{n}$ are also given by Eqs. (4.28)–(4.31), except that the function $N_n(t)$ is now given by

$$N_n(t) = \frac{1}{2\pi}\int_0^\infty A_R(\Omega)\{[n_\Omega(T)+1]\exp(-i\Omega t) + n_\Omega(T)\exp(i\Omega t)\}d\Omega. \tag{4.42}$$

Up to this point we have successfully quantized the problem with an inhomogeneously broadened phonon field.

In the literature, the noise statistics due to the self-Raman effect have been studied using a Hamiltonian approach and the transform of the quantum operator equation into a stochastic equation based on the positive-P representation [16] or the truncated Wigner representation [17]. In those papers, the phonon field is assumed to be purely inhomogeneously broadened, the correlation function is expressed in the Fourier domain, and the nor-

malization units are introduced. Converted into our time domain and expressed in our notation, the correlation function from the expression (12) in Ref. [17] is

$$\bar{N}_n(t) = \frac{1}{2\pi}\int_0^\infty A_R(\Omega)\{[n_\Omega(T)+\tfrac{1}{2}]\exp(-i\Omega t) + [n_\Omega(T)+\tfrac{1}{2}]\exp(i\Omega t)\}d\Omega. \quad (4.43)$$

At first sight, Eq. (4.43) is different from Eq. (4.42). Actually, the two expressions are related to each other by

$$\bar{N}_n(t) = \frac{N_n(t)+N_n(-t)}{2}. \quad (4.44)$$

However, if one further notes that Eq. (3.7) can be put into the form

$$\mathrm{var}[\langle u^A(L,t)|\hat{u}(L,t)\rangle] = \mathrm{var}[\langle u^A(0,t)|\hat{u}(0,t)\rangle] + \int_0^L\int\int Q(z,t_1,t_2)N_n(t_1-t_2)dt_1dt_2dz \quad (4.45)$$

and the function $Q(z,t_1,t_2)$ obeys

$$Q(z,t_1,t_2) = Q(z,t_2,t_1), \quad (4.46)$$

then it is not difficult to see that the calculated quantum uncertainties are the same whether $N_n(t)$ or $\bar{N}_n(t)$ is used. Thus we conclude that the correlation functions derived in this paper agree exactly with the formulation derived in Ref. [17]. Our quantization approach offers an alternative and more straightforward way of quantizing problems and studying noise statistics.

C. Impacts of the self-Raman effect on the squeezing ratio

The formulation in Sec. III can be directly applied to calculate the quantum uncertainties in the presence of the self-Raman effect. The original system after linearization is given by

$$\frac{\partial}{\partial z}\hat{u}(z,t) = id_i\frac{\partial^2}{\partial t^2}\hat{u}(z,t) + 2ik_i|U_0(z,t)|^2\hat{u}(z,t) + ik_iU_0^2(z,t)\hat{u}^\dagger(z,t) + i\int_{-\infty}^t h(t-\tau)|U_0(z,\tau)|^2d\tau\hat{u}(z,t) + iU_0(z,t)\int_{-\infty}^t h(t-\tau)U_0^*(z,\tau)\hat{u}(z,\tau)d\tau + iU_0(z,t)\int_{-\infty}^t h(t-\tau)U_0(z,\tau)\hat{u}^\dagger(z,\tau)d\tau + \hat{n}(z,t). \quad (4.47)$$

The adjoint system is given by

$$\frac{\partial}{\partial z}u^A(z,t) = id_i\frac{\partial^2}{\partial t^2}u^A(z,t) + 2ik_i|U_0(z,t)|^2u^A(z,t) - ik_iU_0^2(z,t)u^{A*}(z,t) + i\int_{-\infty}^t h(t-\tau)|U_0(z,\tau)|^2d\tau u^A(z,t) + iU_0(z,t)\int_t^\infty h(\tau-t)U_0^*(z,\tau)u^A(z,\tau)d\tau - iU_0(z,t)\int_t^\infty h(\tau-t)U_0(z,\tau)u^{A*}(z,\tau)d\tau. \quad (4.48)$$

After backpropagating the adjoint system, the quantum uncertainties between any given weighting function and the perturbed field operator can then be calculated using Eq. (3.7).

As an illustration on how to choose the initial condition for the adjoint system, we utilize the above results to calculate the achievable squeezing ratio in optical fibers in the presence of the self-Raman effect. In squeezing experiments, homodyne detection is usually used for squeezed state detection. We have shown in our previous work [13,14] that the output of the homodyne detection is the inner product of the input field operator and the local oscillator (the projection interpretation of homodyne detection). Therefore the squeezing ratio in squeezing experiments is given by

$$R(L) \equiv \mathrm{var}[\langle f_L(t)|\hat{u}(L,t)\rangle]/\mathrm{var}[\langle f_L(t)|\hat{u}(0,t)\rangle]. \quad (4.49)$$

Here $f_L(t)$ is the local oscillator pulse envelope function. In usual squeezing experiments, one uses the same pulse after propagating through the fiber as the local oscillator, with a possible adjustment of a constant phase. Therefore, the appropriate expression for $f_L(t)$ is

$$f_L(t) = \frac{U_0(L,t)\exp(i\Theta)}{\sqrt{\int|U_0(L,t)|^2dt}}. \quad (4.50)$$

Here Θ is an adjustable phase. One can adjust Θ to minimize the squeezing ratio $R(L)$. To calculate the minimum $R(L)$, one has to backpropagate the adjoint system with two sets of initial conditions. Supposing that with $u^A(L,t) = U_0(L,t)/\sqrt{\int|U_0(L,t)|^2dt}$ the solution of the adjoint system is $u^A(z,t) = F_1(z,t)$ and with $u^A(L,t) = iU_0(L,t)/\sqrt{\int|U_0(L,t)|^2dt}$ the solution of the adjoint system is $u^A(z,t) = F_2(z,t)$, then the squeezing ratio with $u^A(L,t) = f_L(t)$ will be

$$R(L) = A\cos^2\Theta + 2B\cos\Theta\sin\Theta + C\sin^2\Theta. \quad (4.51)$$

Here

$$A = \int |F_1(0,t)|^2 dt + \int_0^L \int_0^L \int\int F_1^*(z,t_1)F_1^*(z',t_2)\langle \hat{n}(z,t_1)\hat{n}(z',t_2)\rangle dt_1 dt_2 dz dz'$$
$$+ \int_0^L \int_0^L \int\int F_1^*(z,t_1)F_1(z',t_2)\langle \hat{n}(z,t_1)\hat{n}^\dagger(z',t_2)\rangle dt_1 dt_2 dz dz'$$
$$+ \int_0^L \int_0^L \int\int F_1(z,t_1)F_1^*(z',t_2)\langle \hat{n}^\dagger(z,t_1)\hat{n}(z',t_2)\rangle dt_1 dt_2 dz dz'$$
$$+ \int_0^L \int_0^L \int\int F_1(z,t_1)F_1(z',t_2)\langle \hat{n}^\dagger(z,t_1)\hat{n}^\dagger(z',t_2)\rangle dt_1 dt_2 dz dz', \tag{4.52}$$

$$B = \frac{1}{2}\int [F_1^*(0,t)F_2(0,t) + F_2^*(0,t)F_1(0,t)]dt$$
$$+\frac{1}{2}\int_0^L \int_0^L \int\int [F_1^*(z,t_1)F_2^*(z',t_2) + F_2^*(z,t_1)F_1^*(z',t_2)]\langle \hat{n}(z,t_1)\hat{n}(z',t_2)\rangle dt_1 dt_2 dz dz'$$
$$+\frac{1}{2}\int_0^L \int_0^L \int\int [F_1^*(z,t_1)F_2(z',t_2) + F_2^*(z,t_1)F_1(z',t_2)]\langle \hat{n}(z,t_1)\hat{n}^\dagger(z',t_2)\rangle dt_1 dt_2 dz dz'$$
$$+\frac{1}{2}\int_0^L \int_0^L \int\int [F_1(z,t_1)F_2^*(z',t_2) + F_2(z,t_1)F_1^*(z',t_2)]\langle \hat{n}^\dagger(z,t_1)\hat{n}(z',t_2)\rangle dt_1 dt_2 dz dz'$$
$$+\frac{1}{2}\int_0^L \int_0^L \int\int [F_1(z,t_1)F_2(z',t_2) + F_2(z,t_1)F_1(z',t_2)]\langle \hat{n}^\dagger(z,t_1)\hat{n}^\dagger(z',t_2)\rangle dt_1 dt_2 dz dz', \tag{4.53}$$

$$C = \int |F_2(0,t)|^2 dt + \int_0^L \int_0^L \int\int F_2^*(z,t_1)F_2^*(z',t_2)\langle \hat{n}(z,t_1)\hat{n}(z',t_2)\rangle dt_1 dt_2 dz dz'$$
$$+ \int_0^L \int_0^L \int\int F_2^*(z,t_1)F_2(z',t_2)\langle \hat{n}(z,t_1)\hat{n}^\dagger(z',t_2)\rangle dt_1 dt_2 dz dz'$$
$$+ \int_0^L \int_0^L \int\int F_2(z,t_1)F_2^*(z',t_2)\langle \hat{n}^\dagger(z,t_1)\hat{n}(z',t_2)\rangle dt_1 dt_2 dz dz'$$
$$+ \int_0^L \int_0^L \int\int F_2(z,t_1)F_2(z',t_2)\langle \hat{n}^\dagger(z,t_1)\hat{n}^\dagger(z',t_2)\rangle dt_1 dt_2 dz dz'. \tag{4.54}$$

The minmum value of $R(L)$ is thus given by

$$\min[R(L)] = \frac{A + C - \sqrt{(A-C)^2 + 4B^2}}{2}. \tag{4.55}$$

Note that in Eqs. (4.52)–(4.54), the integrals needed to be calculated are in fact only three dimensional since all four correlation functions of $\hat{n}$ and $\hat{n}^\dagger$ are δ-function correlated on z. Thus one layer of integrations can be reduced.

Under the assumption of a Lorentzian distribution of the Raman gain and with the set of parameters given in Eqs. (4.12)–(4.15), we calculate the squeezing ratio for 50-fs and 100-fs [full width at half maximum (FWHM)] solitary pulses. The input pulse is the soliton solution in the ideal case [$k_i = \hbar\omega_0 k_0 n_2/A_{\text{eff}}$ and $h(t) = 0$]. It is a sech pulse $A_0\text{sech}(t/\tau_0)$ with $A_0^2\tau_0^2 = 2d_i A_{\text{eff}}/\hbar\omega_0 k_0 n_2$. We did not try to optimize the input pulse shape or the local oscillator pulse shape in the present calculation.

In order to have some idea about the relative magnitudes of different noise sources, in Fig. 1 we plot the squeezing ratio with temperature-dependent noise being ignored. The solid line is the squeezing ratio calculated using the exact propagation equation Eq. (4.8), whereas the dashed line is the squeezing ratio calculated using the approximate propagation equation Eq. (4.9). It can be seen that the approximate model always overestimates the achievable squeezing (i.e., gives a smaller squeezing ratio). The dotted line is the squeezing ratio for ideal solitons (i.e., without the self-Raman effect). It is plotted for comparison. It is interesting to note that even for ideal solitons, the squeezing ratio does not decrease monotonically, but exhibits a small oscillation when it is smaller than 20 dB. This is because once we use the same soliton from the optical fiber as the local oscillator, some parts of the continuum noises will enter the detection [13]. To reject all the continuum noises, an optimum local oscillator pulse shape is needed. The analytical expressions of the optimum local oscillator pulse shape and the optimum squeezing ratio have been derived previously [13]. Actually, one way we checked the accuracy of our calculation was to compare our numerical results for this special case with the analytical results in Ref. [13]. They agree very well. If such an optimum local oscillator pulse shape is used in our calculation, the squeezing ratio for ideal solitons is smaller than the dotted line and decreases monotonically, just as predicted by the analytical theory.

In Fig. 2 we plot the squeezing ratio calculated from

the homogeneously broadened model at 0 K, 77 K, 273 K, 298 K, and 373 K. However, the lines for 0 K and 77 K are too close to be determined from the figure. In Fig. 3, we plot the squeezing ratio calculated from the inhomogeneously broadened model at the same five temperatures. In all the figures the transverse coordinate is the normalized propagation distance in conventional soliton theories [i.e., $\bar{z} = z/z_0$, $z_0 = \tau^2/|k_0''|$, and $\tau = (\text{FWHM})/1.763$].

From the figures, it is clear that the self-Raman effect always increases the squeezing ratio (reduces squeezing). This is not surprising since physically the self-Raman effect causes a soliton frequency downshift and represents additional perturbations to the photon field. However, squeezing still survives even when the self-Raman effect is strong. It is just that the achievable squeezing ratio cannot be made smaller without a limit, at least for the cases considered here. For 50-fs pulses, the lower limit due to transformed original quantum noises is about 14.2 dB [see Fig. 1(a)]. From the inhomogeneously broadened model [see Fig. 3(a)], for 50-fs pulses at 0 K, the lower limit is raised to 11.2 dB. In going from 0 K to 298 K, the lower limit is further raised to 10 dB. For 100-fs pulses, the lower limit due to the transformed original quantum noises is about 21.2 dB [see Fig. 1(b)]. From the inhomogeneously broadened model [see Fig. 3(b)], for 100-fs pulses at 0 K, the lower limit is raised to 18.4 dB. In going from 0 K to 298 K, the lower limit is further raised to 15.6 dB. The prediction from the homogeneous model exhibits a smaller temperature dependence (see Fig. 2), as is expected intuitively. As we have said before, in optical fibers the inhomogeneously broadened mechanisim should dominate. Therefore Fig. 3 instead of Fig. 2 should be used in the comparison with experimental results.

As we have seen, in the presence of the self-Raman effect, as the propagation distance increases, the squeezing ratio will eventually stop decreasing and increase. This behavior is physically different from the saturation of the squeezing ratio at zero group-velocity dispersion [25]. If the dispersion is zero and nonsquare pulses are used, the pulses will get chirped due to self-phase-modulation. The squeezing directions with respect to the phase of the field at different time slots are different since the intensities are different. In homodyne detection, the local oscillator cannot match the squeezing directions at every time slot and thus the squeezing ratio eventually gets saturated. In the case of solitons with the self-Raman effect, the destruction of the squeezing is present even if the temperature-dependent noises introduced midway are ignored (see Fig. 1). This suggests that the nonlinear trans-

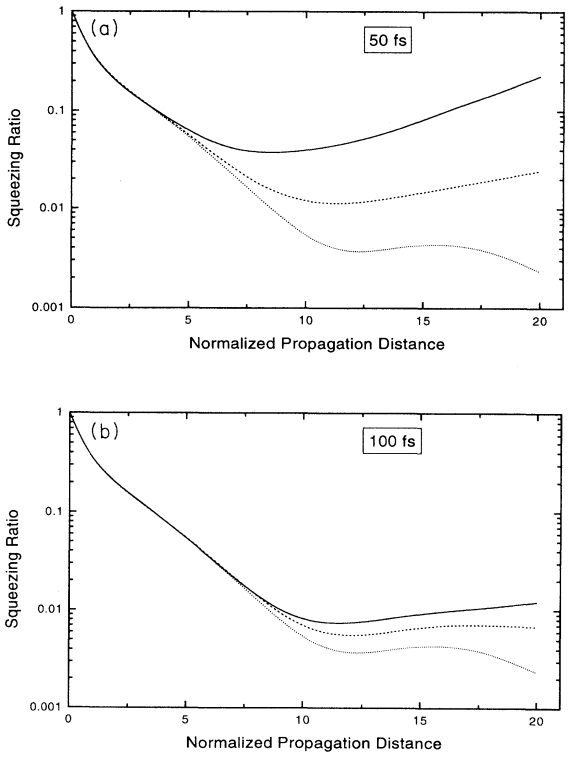

FIG. 1. Squeezing ratio vs normalized propagation distance for (a) 50-fs and (b) 100-fs (FWHM) solitary pulses with the temperature-dependent noise ignored. Solid line, exact propagation equation (4.8), dashed line; approximate propagation equation (4.9); dotted line, ideal solitons. The same pulse after propagating through the fiber is used as the local oscillator.

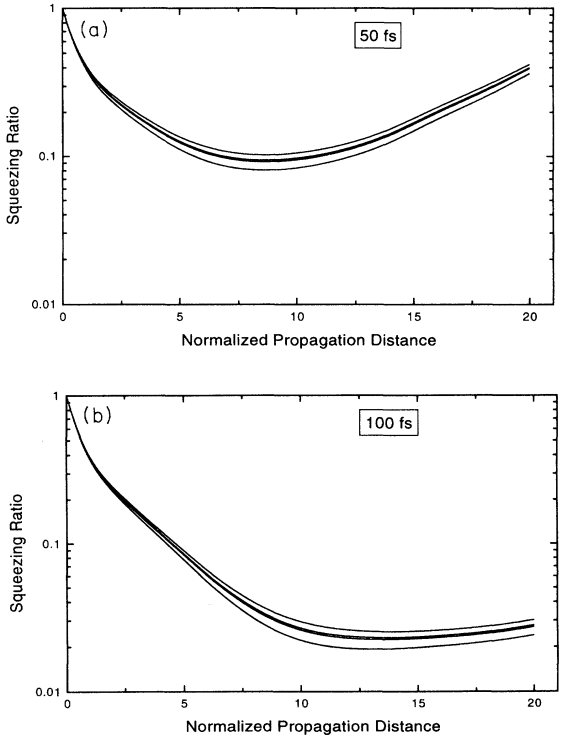

FIG. 2. Squeezing ratio vs normalized propagation distance for (a) 50-fs and (b) 100-fs (FWHM) solitary pulses from the homogeneously broadened model. The lines from the bottom to the top correspond respectively to the squeezing ratios at 0 K, 77 K, 273 K, 298 K, and 373 K. The lines for 0 K and 77 K are too close to be determined. The same pulse after propagating through the fiber is used as the local oscillator.

formation of the self-Raman effect is the main cause for the destruction of squeezing. The nonlinear process of the self-Raman effect changes both the pulse shape and the statistics of the quantum noise. To get maximum squeezing out of the transformed quantum noise may require a special local oscillator pulse shape. However, in our calculation, as well as in real experiments, the final output pulse is used as the local oscillator in the homodyne detection. The contribution from the continuum noises may be increased due to the increased mismatch of the local oscillator pulse shape and the statistics of the quantum noise. In the present paper, we do not try to determine the optimum local oscillator pulse shape or the optimum input pulse shape in order to achieve the biggest observed squeezing. However, as a primary investigation, we have tried the sech local oscillator pulse shape and the optimum local oscillator pulse shape given in Ref. [13] for ideal solitons (i.e., without the self-Raman effect). The calculated squeezing ratio for 100-fs solitons at 77 K is shown in Fig. 4. It can be seen that with the optimum local oscillator pulse shape given for ideal solitons, the squeezing ratio is indeed smaller when the normalized propagation distance is less than 8. However, when the normalized propagation distance is further increased, the squeezing ratio gets even larger. This clearly shows that the optimum local oscillator pulse shape for ideal solitons is no longer optimum in the presence of the self-Raman effect.

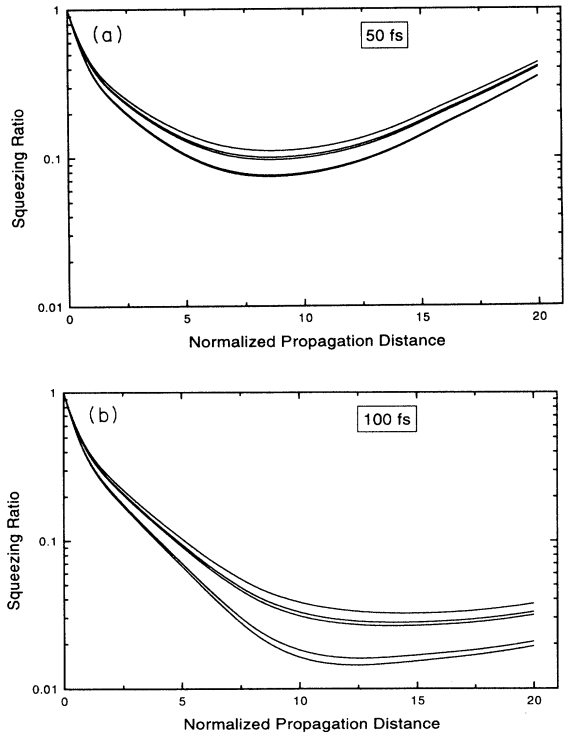

FIG. 3. Squeezing ratio vs normalized propagation distance for (a) 50-fs and (b) 100-fs (FWHM) solitary pulses from the inhomogeneously broadened model. The lines from the bottom to the top correspond respectively to the squeezing ratios at 0 K, 77 K, 273 K, 298 K, and 373 K. The same pulse after propagating through the fiber is used as the local oscillator.

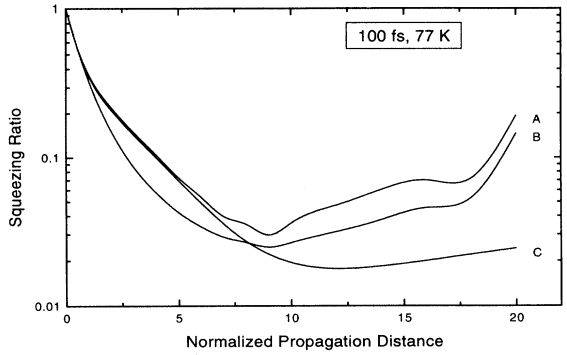

FIG. 4. Squeezing ratio vs normalized propagation distance for 100-fs (FWHM) solitary pulses at 77 K from the inhomogeneously broadened model: curve A, with the sech local oscillator pulse shape; curve B, with the optimum local oscillator pulse shape given in Ref. [13] for ideal solitons; curve C, with the pulse after propagating through the fiber as the local oscillator.

In real squeezing experiments, additional noises due to processes such as guided acoustic wave Brillouin scattering (GAWBS) [23,24] will also show up. Physically, GAWBS can be modeled in the same way as in the inhomogeneously broadened case, except that GAWBS has different resonance frequencies, different coupling strengths, and different relaxation rates. As long as these characteristics are determined, they can be easily incorporated in the calculation. Nevertheless, since we do not include these noises in the present calculation, the results given in this paper represent the ideal lower limit of the squeezing ratio for squeezing experiments using optical fibers.

In real squeezing experiments, a periodic pulse train is used, whereas the theoretical calculation is performed for a single pulse. When the time separation between two adjacent pulses is longer than the time for the phonon field to reach thermal equilibrium again, then the temperature of the phonon field is equal to the environment temperature. However, if the time separation between two adjacent pulses is shorter than the time for the phonon field to reach thermal equilibrium, then the actual temperature of the phonon field may be higher than the environment temperature. This may cause some ambiguity in comparing experimental results with theoretical prediction and needs to be investigated more carefully. One recent experiment at 1.3 μm [3] actually utilized a pulse train with a high pulse repetition rate to reduce GAWBS noises. Calculation of the squeezing ratio for a periodic pulse train instead of a single pulse is another possible research topic to be addressed in the future.

V. CONCLUSIONS

A general method has been developed for quantizing and solving nonlinear optical pulse propagation problems. The quantization is performed on the linearized

equation and noise operators are introduced to preserve the commutation brackets. Quantum uncertainties of the inner product of any given function and the perturbed field operator are calculated by backpropagating the adjoint system. The formulation is very elegant and applicable to general nonlinear optical pulse propagation problems. We have developed a self-consistent quantum theory of the self-Raman effect in optical fibers and use it to study the influence of the self-Raman effect on soliton squeezing. We are now investigating more complicated nonlinear pulse propagation problems based on our general theory.

ACKNOWLEDGMENTS

One of the authors (Y.L.) would like to acknowledge private communication with Professor H. A. Haus at Massachusetts Institute of Technology. The work was supported by the National Science Council of the Republic of China (ROC) under Contract No. NSC 83-0417-E-009-003. The authors also want to thank the National Center for High-Performance Computing of the ROC for offering us their computational power.

APPENDIX

In this appendix we prove that by introducing noise operators according to Eqs. (2.7)–(2.9), the commutation relations Eqs. (2.4) and (2.5) are correct for all z. The reasoning is as follows. Supposing Eqs. (2.4) and (2.5) are correct at z, we are going to show that they are also correct at $z + dz$.

From Eq. (2.6) we have, to first order of dz,

$$\hat{u}(z+dz,t)=\hat{u}(z,t)+\{P_1(z,t)\hat{u}(z,t)+P_2(z,t)\hat{u}^\dagger(z,t)\}dz+\int_z^{z+dz}\hat{n}(z',t)dz'. \tag{A1}$$

Moreover,

$$\{[\hat{u}(z+dz,t_1),\hat{u}^\dagger(z+dz,t_2)]-[\hat{u}(z,t_1),\hat{u}^\dagger(z,t_2)]\}/dz$$

$$=[\hat{u}(z,t_1),P_1^*(z,t_2)\hat{u}^\dagger(z,t_2)]+[P_1(z,t_1)\hat{u}(z,t_1),\hat{u}^\dagger(z,t_2)]+\frac{1}{dz}\int_z^{z+dz}\int_z^{z+dz}[\hat{n}(z',t_1),\hat{n}^\dagger(z'',t_2)]dz'dz''$$

$$=\{P_1(z,t_1)+P_1^*(z,t_2)\}\delta(t_1-t_2)+N(z,t_1,t_2). \tag{A2}$$

Equation (A2) has to be zero. This tells us what the correct $N(z,t_1,t_2)$ is. Just to be sure, we also check if $[\hat{u}(z,t_1),\hat{u}(z,t_2)]$ is preserved

$$\{[\hat{u}(z+dz,t_1),\hat{u}(z+dz,t_2)]-[\hat{u}(z,t_1),\hat{u}(z,t_2)]\}/dz$$

$$=[P_2(z,t_1)\hat{u}^\dagger(z,t_1),\hat{u}(z,t_2)]+[\hat{u}(z,t_1),P_2(z,t_2)\hat{u}^\dagger(z,t_2)]=-P_2(z,t_1)\delta(t_2-t_1)+P_2(z,t_2)\delta(t_1-t_2). \tag{A3}$$

At first sight, one may think that this is not necessarily equal to zero in general. However, please remember that the δ function has real meaning only when it is inserted inside integrals. Using Eq. (A3), it is easy to prove that

$$\left[\int f^*(t_1)\hat{u}(z,t_1)dt_1,\int f^*(t_2)\hat{u}(z,t_2)dt_2\right] \tag{A4}$$

are independent of z for *any* given function $f(t)$.

[1] M. Rosenbluh and R. M. Shelby, Phys. Rev. Lett. **66,** 153 (1991).
[2] K. Bergman and H. A. Haus, Opt. Lett. **16,** 663 (1991).
[3] K. Bergman, H. A. Haus, E. P. Ippen, and M. Shirasaki, Opt. Lett. **19,** 290 (1993).
[4] M. Shirasaki and H. A. Haus, J. Opt. Soc. Am. B **7,** 30 (1990).
[5] K. J. Blow, R. Loudon, and S. J. D. Phoenix, Phys. Rev. A **45,** 8064 (1992).
[6] F. X. Kartner, L. G. Jonechis, and H. A. Haus, Quantum Opt. **4,** 379 (1992).
[7] L. G. Jonechis and J. H. Shapiro, J. Opt. Soc. Am. B **10,** 1102 (1993).
[8] S. J. Carter, P. D. Drummond, M. D. Reid, and R. M. Shelby, Phys. Rev. Lett. **58,** 1841 (1987).
[9] P. D. Drummond and S. J. Carter, J. Opt. Soc. Am. B **4,** 1565 (1987).
[10] P. D. Drummond, S. J. Carter, and R. M. Shelby, Opt. Lett. **14,** 373 (1989).
[11] Y. Lai and H. A. Haus, Phys. Rev. A **40,** 844 (1989).
[12] Y. Lai and H. A. Haus, Phys. Rev. A **40,** 854 (1989).
[13] H. A. Haus and Y. Lai, J. Opt. Soc. Am. B **7,** 386 (1990).
[14] Y. Lai, J. Opt. Soc. Am. B **10,** 475 (1993).
[15] F. Singer, M. J. Potasek, J. M. Fang, and M. C. Teich, Phys. Rev. A **46,** 4192 (1992).
[16] S. J. Carter and P. D. Drummond, Phys. Rev. Lett. **67,**

3757 (1991).
[17] P. D. Drummond and A. D. Hardman, Europhys. Lett. **21,** 279 (1993).
[18] Y. Lai and H. A. Haus, Phys. Rev. A **42,** 2925 (1990).
[19] Y. Yamamoto and H. A. Haus, Rev. Mod. Phys. **58,** 1001 (1986).
[20] Y. Lai, IEEE J. Lightwave Technol. **11,** 462 (1993).
[21] J. P. Gordon, Opt. Lett. **11,** 662 (1986).
[22] R. H. Stolen, J. P. Gordon, W. J. Tomlinson, and H. A. Haus, J. Opt. Soc. Am. B **6,** 1159 (1989).
[23] R. M. Shelby, M. D. Levenson, and P. W. Bayer, Phys. Rev. B **31,** 5244 (1985).
[24] R. M. Shelby, P. D. Drummond, and S. J. Carter, Phys. Rev. A **42,** 2966 (1990).
[25] K. Bergman, H. A. Haus, and Y. Lai, J. Opt. Soc. Am. B **8**, 1952 (1991).